11th Australasian Fluid Mechanics Conference
University of Tasmania, Hobart, Australia
14-18 December 1992

NUMERICAL SIMULATION OF FLOW PAST AN ELLIPTIC CYLINDER AT MODERATE AND HIGH REYNOLDS NUMBERS, USING A SPECTRAL METHOD

Yoshihiro MOCHIMARU

Department of Mechanical Engineering
Tokyo Institute of Technology, Tokyo 152, JAPAN

ABSTRACT

Steady-state two-dimensional laminar incompressible flow past an elliptic cylinder placed normally to a uniform flow and parallel to the major axis is analized numerically. Using a Fourier spectral method through substantially doubly exponential transformation in space, the equation of vorticity transport can be integrated to give a steady-state solution through a time marching way even for a relatively high Reynolds number. Not only drag coefficients and streamlines but also isobars are presented. Decrease in drag coefficients in a higher Reynolds number region is shown as is expected experimentally.

NOTATION

a	semi-major axis
b	semi-minor axis $= a \tanh \alpha_0$
C_D	drag coefficient = drag per unit depth / $(\rho U_\infty^2 a)$
L	length of perimeter of the elliptic section
p	pressure
Re	Reynolds number $= aU_\infty/\nu$
Re_D	Reynolds number based on the minor axis $= 2Re \times (b/a)$
s	arc length measured from the forward stagnation point
t	time
U_∞	free stream velocity
x	Cartesian coordinate
y	Cartesian coordinate
α	elliptic coordinate defined in Eq.(1)
α_0	elliptic coordinate corresponding to the surface of the cylinder $= \tanh^{-1}(b/a)$
β	elliptic coordinate defined in Eq.(1)
ζ	dimensionless vorticity
ν	kinematic viscosity
ρ	density of fluid
ψ	dimensionless stream function

INTRODUCTION

Flow past an elliptic cylinder is one of fundamental flows past a cylinder, so that flow characteristics were widely investigated, e.g., experimentally by Prandtl and Tietjens (1957), Zahm et al.(1928), Richards (1934), and numerically by Mochimaru (1990). In this paper, a new method is developed to support a relatively high Reynolds number region for a two-dimensional steady laminar flow field past an elliptic cylinder placed normally to a uniform flow, the direction of which is assumed to be parallel to the major axis of the elliptic section.

ANALYSIS

Basic Equations

Fluid is assumed to be Newtonian and incompressible, and viscosity is assumed to be constant. Hereafter it is assumed that length, velocity, pressure, and time are made dimensionless with respect to the semi-major axis a (of the elliptic section), free stream velocity U_∞, ρU_∞^2, and a/U_∞ respectively. Let (x, y, z) be a Cartesian coordinate system such that the z-axis coincides with the central axis of the elliptic cylinder and that the direction of the positive x-axis is that of the uniform flow. Let (α, β) be an elliptic coordinate system (in the xy-plane) such that $\alpha = \alpha_0 (> 0)$ corresponds to the surface of the cylinder. Thus

$$x + iy = \cosh(\alpha + i\beta) / \cosh \alpha_0 \,. \tag{1}$$

Then the equation of vorticity transport can be expressed as

$$\frac{1}{2\cosh^2 \alpha_0} (\cosh 2\alpha - \cos 2\beta) \frac{\partial \zeta}{\partial t} + \frac{\partial(\zeta, \psi)}{\partial(\alpha, \beta)}$$

$$= \frac{1}{Re} \left(\frac{\partial^2}{\partial \alpha^2} + \frac{\partial^2}{\partial \beta^2} \right) \zeta \,, \tag{2}$$

where ζ is a non-zero component of vorticity, and is given through a stream function by

$$\frac{1}{2\cosh^2 \alpha_0} (\cosh 2\alpha - \cos 2\beta) \zeta = - \left(\frac{\partial^2}{\partial \alpha^2} + \frac{\partial^2}{\partial \beta^2} \right) \psi \,. \tag{3}$$

Fluid Flow Behaviour Far From The Cylinder Under A Steady State

Asymptotic behaviour of steady fluid flow far from the cylinder is expressed as

$$\psi(\alpha_\infty, \beta) = \frac{\exp \alpha_\infty}{2\cosh \alpha_0} \sin \beta + \frac{1}{2} C_D \left(\frac{\beta}{\pi} - \operatorname{erf} Q \right), \tag{4}$$

$$\zeta(\alpha_\infty, \beta) = - \frac{C_D Re}{\sqrt{\pi}} \exp(-\alpha_\infty) \cosh \alpha_0 \; Q \exp\left(-Q^2\right), \tag{5}$$

$$Q = \left(\frac{Re \exp \alpha_\infty}{2\cosh \alpha_0} \right)^{1/2} \sin\left(\frac{\beta}{2}\right), \tag{6}$$

where $\exp(\alpha_\infty) \gg 1$, and $-\pi < \beta \leq \pi$.

Boundary Conditions At The Surface Of The Cylinder

No-slip conditions are specified. That is,

$$\psi(\alpha = \alpha_0) = 0 , \tag{7}$$

$$\frac{\partial \psi}{\partial \alpha}(\alpha = \alpha_0) = 0 . \tag{8}$$

NUMERICAL SOLUTION PROCEDURE

Primary Variables

The stream function ψ and vorticity ζ can be expanded into the following Fourier series of β :

$$\psi = \sum_{n=1}^{\infty} \psi_n(\alpha, t) \sin n\beta , \tag{9}$$

$$\zeta = \sum_{n=1}^{\infty} \zeta_n(\alpha, t) \sin n\beta . \tag{10}$$

Then, using the addition formulae of trigonometric functions, Eqs.(2) and (3) can be separated into each Fourier component of β, which constitutes a set of differential equations for ψ_n 's and ζ_n 's in α and t in the interior region ($\alpha_0 < \alpha < \alpha_\infty$) [a kind of a Fourier spectral method.] As an example shown are the 1st components of Eqs.(2) and (3):

$$\frac{1}{2\cosh^2 \alpha_0}\left\{\left(\cosh 2\alpha + \frac{1}{2}\right)\frac{\partial \zeta_1}{\partial t} - \frac{1}{2}\frac{\partial \zeta_3}{\partial t}\right\}$$

$$+\frac{1}{2}\sum_{n=1}^{\infty} n\left\{\psi_n \frac{\partial}{\partial \alpha}\zeta_{n+1} - \zeta_n \frac{\partial}{\partial \alpha}\psi_{n+1}\right\}$$

$$-\frac{1}{2}\sum_{n=2}^{\infty} n\left\{\psi_n \frac{\partial}{\partial \alpha}\zeta_{n-1} - \zeta_n \frac{\partial}{\partial \alpha}\psi_{n-1}\right\} = \frac{1}{Re}\left(\frac{\partial^2}{\partial \alpha^2} - 1\right)\zeta_1 , \tag{11}$$

$$\frac{1}{2\cosh^2 \alpha_0}\left\{\left(\cosh 2\alpha + \frac{1}{2}\right)\zeta_1 - \frac{1}{2}\zeta_3\right\} = -\left(\frac{\partial^2}{\partial \alpha^2} - 1\right)\psi_1 \tag{12}$$

respectively.

Boundary Conditions At The Surface ($\alpha = \alpha_0$)

Equation (8) can be replaced by

$$\frac{2}{h^2}\psi(\alpha = \alpha_0 + h) + \frac{\cosh 2\alpha_0 - \cos 2\beta}{2\cosh^2 \alpha_0}\zeta(\alpha = \alpha_0 + h) = 0 , \tag{13}$$

where $\alpha_0 + h$ is the coordinate at the adjacent grid to the cylinder surface. Thus Eq.(7) can be separated to give

$$\psi_n(\alpha = \alpha_0) = 0 \quad (n \geq 1) . \tag{14}$$

Substituting Eqs.(9) and (10) into Eq.(13) gives

$$\frac{2}{h^2}\psi_n + \frac{1}{2\cosh^2 \alpha_0}\left(\cosh 2\alpha_0 \, \zeta_n - \frac{1}{2}\zeta_{n-2} - \frac{1}{2}\zeta_{n+2}\right) = 0 , \tag{15}$$

where $n \geq 3$, and

$$\frac{2}{h^2}\psi_1 + \frac{1}{2\cosh^2 \alpha_0}\left(\cosh 2\alpha_0 \, \zeta_1 - \frac{1}{2}\zeta_3 + \frac{1}{2}\zeta_1\right) = 0 , \tag{16}$$

$$\frac{2}{h^2}\psi_2 + \frac{1}{2\cosh^2 \alpha_0}\left(\cosh 2\alpha_0 \, \zeta_2 - \frac{1}{2}\zeta_4\right) = 0 . \tag{17}$$

Throughout Eqs.(15) $\sim$ (17), values of ψ_n 's and ζ_n 's are evaluated at $\alpha = \alpha_0 + h$.

Virtual Boundary Conditions At $\alpha = \alpha_\infty$

The coefficient C_D is given by

$$C_D = \frac{\pi}{Re}\left(\tanh \alpha_0 \frac{\partial}{\partial \alpha}\zeta_1 - \zeta_1\right)_{\alpha = \alpha_0} . \tag{18}$$

Thus Eqs.(4) and (5) can be expanded into Fourier series of β at least numerically.

Numerical Integration Scheme

A set of simultaneous algebraic equations can be formed by truncating the series (9) and (10) up to a certain order, and by discretizing the resulting system of differential equations, e.g. Eq.(11), in space α and time t by a finite difference method, incorporated with boundary conditions, where to support cases of a relatively high Reynolds number introduced is non-uniform grid spacing in the α -coordinate (substantially doubly exponential transformation in the physical plane far from the cylinder); that is, the coordinate α_n for the n -th grid point (numbered from the surface of the cylinder; n=0 on the surface) is defined as

$$\alpha_n = \alpha_0 + h\left\{\frac{\sinh\,(n-1)\gamma}{\sinh \gamma} + 1\right\} , \tag{19}$$

where γ is a suitable positive constant to be chosen. This produces grids with finer spacing near the surface of the cylinder. The case $\gamma \to 0$ corresponds to a uniform grid spacing in α (substantially exponential transformation in the physical space), and the larger the Reynolds number, the smaller h should be. Discretization in space by a finite difference approximation can be based on accuracy of the order of h . Then the system of equations can be integrated with respect to time by a time marching way, using a semi-implicit method, to give a steady-state solution, where as initial values a potential flow field is assumed, being superimposed with an approximate developing boundary-layer flow field keeping only a $\sin\beta$ component. Each pair of the functions, ψ_n and ζ_n , possessing the same suffixes may be solved separately at every time step. Boundary conditions far from the cylinder at intermediate time are treated as Mochimaru(1989).

NUMERICAL RESULTS

Drag coefficients

Drag coefficients C_{DN} (which is defined as the standard one based on dynamic pressure and projection area; $= C_D \times (a/b)$) are shown in Figs.1,2, and 3 for $b/a = 1/3$, $1/12$, and $1/2$ respectively. Remarkable reduction of drag coefficients in the higher Reynolds number region can be found in Fig.1.

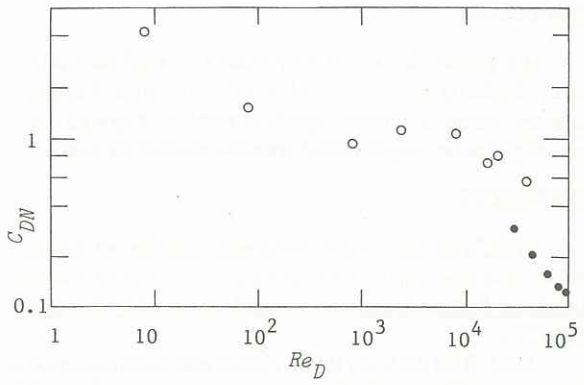

Fig.1 Drag coefficients for $b/a = 1/3$. ○ : present numerical data, ● : experimental data by Zahm et al.

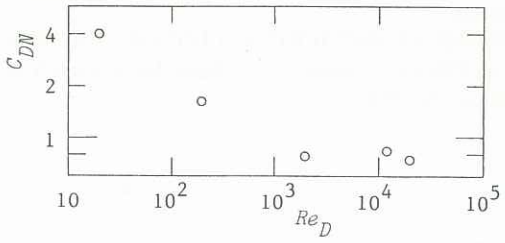

Fig.2 Drag coefficients for $b/a = 1/12$. ○: present numerical data.

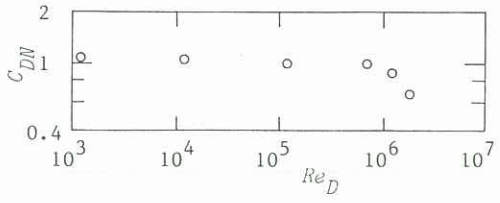

Fig.3 Drag coefficients for $b/a = 1/2$. ○: present numerical data.

Flow Pattern

Streamlines near the trailing edge are shown in Fig.4 at $Re_D = 40000$ for $b/a = 1/6$.

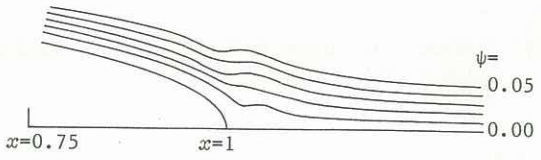

Fig.4 Streamlines in the upper half plane near the trailing edge at $Re_D = 40000$, $b/a = 1/6$.

Pressure Fields

Pressure p itself can be obtained from the following total differential equation:

$$\mathrm{d}\left[p + \frac{1}{2}\left\{\left(\frac{\partial\psi}{\partial x}\right)^2 + \left(\frac{\partial\psi}{\partial y}\right)^2\right\}\right]$$

$$= -\zeta\frac{\partial\psi}{\partial x}\mathrm{d}x - \zeta\frac{\partial\psi}{\partial y}\mathrm{d}y + \frac{1}{Re}\left(\frac{\partial\zeta}{\partial x}\mathrm{d}y - \frac{\partial\zeta}{\partial y}\mathrm{d}x\right), \qquad (20)$$

where gravity is neglected. Isobars are shown in Figs.5, 6, and 7 at $Re_D = 400$, $Re_D = 10000$, and $Re_D = 40000$ for $b/a = 1/6$ respectively, the latter two being limited in the vicinity of the trailing edge. In case of high Reynolds number flows, pressure $p - p_\infty$ (p_∞ : pressure at the free stream) along the symmetrical axis in the wake region is mostly negative as in Figs.6 and 7. Pressure distribution along the perimeter is shown in Fig.8 for $Re_D = 400$, $b/a = 1/6$.

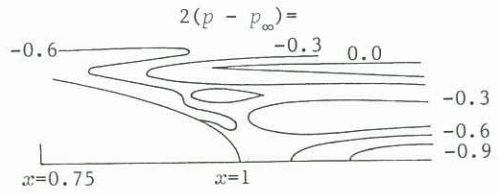

Fig.6 Isobars in the upper half plane near the trailing edge at $Re_D = 10000$, $b/a = 1/6$.

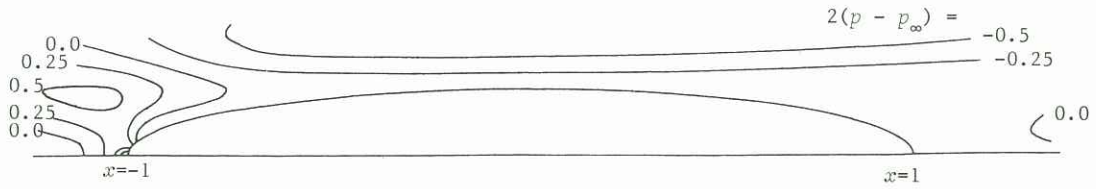

Fig.5 Isobars in the upper half plane at $Re_D = 400$, $b/a = 1/6$. Fluid flows from left to right.

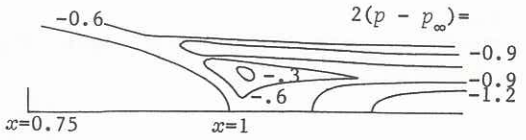

Fig.7 Isobars in the upper half plane near the trailing edge at $Re_D = 40000$, $b/a = 1/6$.

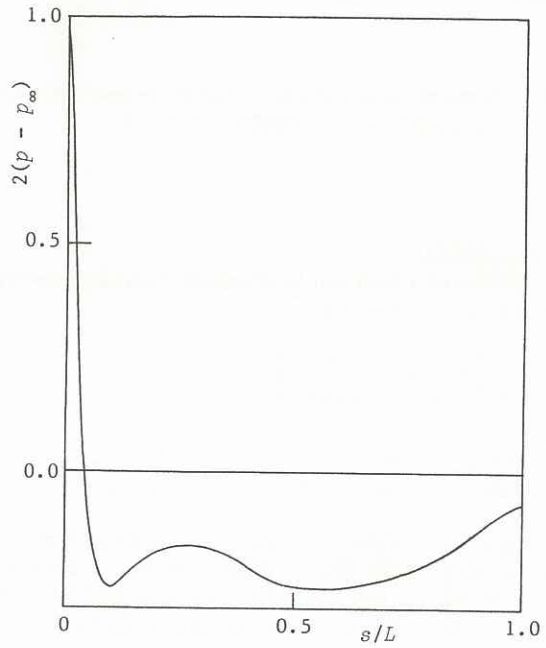

Fig.8 Pressure distribution along the perimeter at $Re_D = 400$, $b/a = 1/6$.

CONCLUSION

It is found that the steady-state flow field past an elliptic cylinder is well simulated at relatively high Reynolds numbers, using a Fourier spectral method through substantially doubly exponential tramsformation in space.

REFERENCES

MOCHIMARU,Y(1989)Natural and forced convection from a horizontal circular cylinder to liquid metals. Numerical Methods in Laminar and Turbulent Flow,6-2, 1207-1215.

MOCHIMARU,Y(1990) Numerical simulation of a flow past an elliptic cylinder at low and moderate Reynolds numbers. Proc.The 2nd KSME-JSME Fluids Eng.Conf., Seoul, 1,424-429.

PRANDTL,L and TIETJENS,OG(1957)Applied Hydro- and Aeromechanics, Dover Pub., New York, 305-307.

RICHARDS,GJ(1934)On the motion of an elliptic cylinder through a viscous fluid. Phil.Trans.Soc.Lond., A, 233,279-301.

ZAHM,AF,SMITH,RH, and LOUDEN,FA(1928) Forces on Elliptic Cylinder in Uniform Air Stream.NACA Tech. Rept. No.289.